European Journal of Radiology Open 8 (2021) 100355

Contents lists available at ScienceDirect

European Journal of Radiology Open

journal homepage: www.elsevier.com/locate/ejro

Diffusion-weighted MRI and FLAIR sequence for differentiation of hydatid cysts and simple cysts in the liver

Kursad Yalcinoz [a], Turkan Ikizceli [b,*], Servet Kahveci [c], Okkes Ibrahim Karahan [d]

[a] Elbistan State Hospital, Radiology Clinic, Kahramanmaras, Turkey
[b] University of Health Sciences, Istanbul Haseki Training and Research Hospital, Department of Radiology, Adnan Adivar Street, Number: 9, 34130, Fatih, Istanbul, Turkey
[c] Umm Slal Health Center, Doha, Qatar
[d] Erciyes University, Department of Radiology, Kayseri, Turkey

HIGHLIGHTS

- DWI signal characteristics are useful in differentiating between hydatid cysts and simple cysts.
- ADC values (b600 and b1000) can distinguish hydatid cyst and simple cyst.
- FLAIR sequence contributes to the differentiation of type 2 hydatid and simple cysts.

ARTICLE INFO

Keywords:
Diffusion-weighted imaging
Apparent diffusion coefficient
FLAIR
Hydatid cyst
Simple cyst

ABSTRACT

Purpose: The contribution of DWI and FLAIR to the differential diagnosis of type 1, 2, and 3 hydatid cysts and simple liver cysts was investigated according to the Gharbi classification. This study is the first report using FLAIR sequence for the differential diagnosis of liver hydatid cysts in this regard.
Methods: A total of 82 hydatid cysts and 40 simple cysts were scanned with DWI (in b600-b1000 values) and FLAIR sequence. In 64 patients included in the study, a total of 122 cystic lesions were diagnosed histopathologically or during follow-up. FLAIR and DWI signal characteristics were evaluated, and ADC values were calculated.
Results: The mean ADC value of hydatid cysts on DWI (b600) was $3.07 \pm 0.41 \times 10^{-3}$ s/mm^2, while it was $3.91 \pm 0.51 \times 10^{-3}$ s/mm^2 for simple cysts and the difference was statistically significant ($p < 0.05$). On b1000 DWI, the mean ADC values of hydatid and simple cysts were $2.99 \pm 0.38 \times 10^{-3}$ s/mm^2 and $3.43 \pm 0{:}29 \times 10^{-3}$ s/mm^2, respectively ($p < 0.05$). The qualitative evaluation of the signal intensity on b600−1000 DWI demonstrated the difference between the simple and hydatid cyst groups ($p < 0.05$). Type 2 hydatid cysts alone were distinguished from type 2–3 hydatid and simple cysts by FLAIR ($p < 0.05$).
Conclusions: ADC values can distinguish between hydatid cyst and simple cyst. FLAIR contributes to the differentiation of type 2 hydatid and simple cysts.

1. Introduction

Hydatid cyst of the liver still continues to be an important public health problem in developing countries [1]. Hydatid cyst often remains silent for a lifetime and does not cause clinical symptoms. But if clinical symptoms exist, blunt right upper quadrant pain is the most common complaint in patients. Weakness, fever, dyspepsia, and nausea are the other nonspecific findings. In complicated hydatid cysts, fever, jaundice, and rarely anaphylactic reactions can be seen. The diagnosis is mostly made incidentally as a result of imaging procedures performed for another reason. Approximately 50–70 % of cysts settle in the liver [2]. They were classified by Gharbi in 1981 [3]. Recently, in 2003, the World Health Organization (WHO) Informal Working Group on Echinococcus updated a new classification of cystic echinococcosis based on

* Corresponding author.
E-mail addresses: kursadyalcinoz@hotmail.com (K. Yalcinoz), turkan.ikizceli@sbu.edu.tr (T. Ikizceli), servetkahveci@hotmail.co.uk (S. Kahveci), oikarahan@yahoo.com (O.I. Karahan).

https://doi.org/10.1016/j.ejro.2021.100355
Received 19 March 2021; Received in revised form 6 May 2021; Accepted 8 May 2021

ultrasonographic findings of hepatic hydatid cyst. Abdel Razek et al. published a new version of the WHO classification based on magnetic resonance imaging (MRI) findings in 2009 [4–6]. Among the imaging methods, ultrasonography (US) especially is an easily accessible method that should be applied first [7,8]. Computed tomography and MRI often offer the possibility to better define anatomic relations. MRI is also used for diagnosis and treatment follow-up in some centers [9].

Diffusion-weighted imaging (DWI) is a method sensitive to molecular diffusion in tissues and is widely used in brain imaging. Müller et al. first used diffusion MRI for focal and diffuse diseases of the liver, spleen, renal lesions, and muscle tissue, and obtained significant results [10]. In the following years, many researchers published studies about the applications of DWI in the liver, kidneys, and other abdominal organs [11, 12]. However, there are a limited number of studies investigating the role of DWI in hydatid cyst disease of the liver [13,14].

Fluid-attenuated inversion recovery (FLAIR), which is an inversion recovery (IR) sequence, is one of the routine sequences in neuroradiology. This special sequence removes the signal from cerebrospinal fluid in the resulting images. Cerebral tissues on FLAIR appear similar to T2-WI with gray matter brighter than white matter but fluids are dark instead of appearing white. Due to this high sensitivity and excellent suppression of the cerebrospinal fluid signal, FLAIR is used routinely for neuroimaging [15].

In this study, the contribution of DWI and FLAIR sequences to the differential diagnosis of type 1, 2, and 3 hydatid cysts and simple liver cysts according to the Gharbi classification was investigated. This study is the first report using the FLAIR sequence for the differential diagnosis of liver hydatid cysts.

2. Methods

2.1. Patient selection

After approval from Erciyes University Clinical Research Ethics Committee (2012/79), the study included patients with liver hydatid cyst (type 1, 2, 3) or simple cyst previously detected by US and computed tomography retrospectively. After the informed consent form was obtained, an MRI examination including FLAIR sequence and DWI was performed. Hydatid cysts were classified according to the Gharbi classification, and type 1, 2, and 3 hydatid cysts were included in the study. Type 4 hydatid cysts were excluded from the study due to their solid character and type 5 hydatid cysts are solid and contain peripheral calcification. Cysts smaller than 2 cm were excluded because of the limit of DWI resolution. Patients with hydatid cysts who could not tolerate MRI and simple cyst cases without long-term follow-up were excluded from the study.

Of the 64 patients (27 men, 37 women) included in the study, 22 patients had a total of 40 simple cysts, and 42 patients had a total of 82 hydatid cysts (122 cystic lesions in total). While 10 of 40 simple cysts were diagnosed histopathologically as a result of surgical operations, 30 simple cysts were diagnosed as serologically negative, radiological findings were in favor of simple cysts, and no size change was seen in US follow-up. Histopathological diagnosis was made after percutaneous aspiration for 46 hydatid cysts out of 82 hydatid cysts and 36 hydatid cysts after surgical operation.

2.2. Imaging technique

Routine upper abdominal MRI was performed using a 1.5 T MRI device (Philips Gyroscan Intera, Best, The Netherlands) with a 4-phase channel body coil. For routine examination, axial and coronal T2-weighted single-shot turbo spin-echo (TSE) (TR/TE 700/80, FA: 90°, slice thickness 7 mm, gap 1 mm, FOV: 35−40 cm) and axial T2-weighted TSE with fat-suppression, T1-weighted gradient dual-echo (in phase and out of phase) (TR/TE 80/4.2−3.6, FA: 80°, slice thickness 7 mm), axial T1-weighted spoiled gradient-echo (fast-field echo [FFE]) images with and without fat suppression (TR /TE: 169/4, FA: 80°, matrix: 256 × 128, slice thickness 7 mm, gap 1 mm) and FLAIR sequence (TR/TE 6000/120, TI: 2000, slice thickness 7 mm, gap 1 mm) were obtained. Fat suppression was obtained using the spectral pre-saturation with inversion recovery (SPIR) technique. DWI was obtained by applying diffusion sensitive gradients at different b values (b0, b600, b1000sec/mm^2) in the axial plane in single-shot spin-echo echo-planar sequence (TR 3656 mms, TE 89 mms (b1000), TR 2673, TE 60 (b600), matrix: 256 × 128, FOV 35−40 cm, slice thickness 7 mm, interslice gap 1 mm). Fat-suppressed pulses were used to avoid serious chemical-shift artifacts. ADC maps of isotropic images were created automatically by the device. ADC values for the lesions were calculated on ADC maps created in the second MRI console (View Forum R5.x, Philips Medical Systems). After DWI, contrast-enhanced dynamic imaging was obtained with an axial gradient-echo T1-weighted MRI sequence after the administration of gadopentetate dimeglumine at a dose of 0.1 mmol/kg of body weight as a bolus injection of 25 s (arterial), 60 s (portal), 120 s (equilibrium), and 5 min. The MRI parameters used are summarized in Table 1.

Table 1
Imaging parameters on a 1.5 T magnet scanner.

Sequences	Parameters
Axial and coronal T2-weighted sing-shot TSE	TR/TE 700/80, FA: 90°, slice thickness 7 mm, gap 1 mm, FOV: 35−40 cm
Axial T2-weighted TSE with fat-suppression	TR/TE 700/80
Axial T1-weighted gradient dual-echo	TR/TE 80/4.2−3.6, FA: 80°, slice thickness 7 mm
Axial T1-weighted spoiled gradient-echo (FFE)	TR /TE: 169/4, FA: 80°, matrix: 256 × 128, slice thickness 7 mm, gap 1 mm
FLAIR	TR/TE 6000/120, TI: 2000, slice thickness 7 mm, gap 1 mm

TR/TE: repetition time/echo time, FOV: Field of view, FA: Flip Angle, TSE: Turbo Spin Echo, FFE: Fast-Field Echo, FLAIR: Fluid-Attenuated Inversion Recovery, TI: Time Inversion.

2.3. Image analysis

The sizes of the cysts were recorded. Cyst signal intensity on DWI was evaluated as isointense, peripheral hyperintense, moderately hyperintense, and hyperintense compared to liver parenchyma. The measurements were made by placing the region of interest (ROI) on the cysts covering 2/3 of the lesion. If there was an image of the lesion in consecutive sections, ADC measurements were made from these, and the average ADC value was calculated. The average ADC values were measured, and the diagnoses of the patients were compared.

Cyst signal intensity was classified as hypointense, isointense, and hyperintense compared to liver parenchyma on FLAIR images.

All evaluations were qualitatively and quantitatively evaluated for each cyst by an academic radiologist (20 years' experience) unaware of the final diagnosis.

2.4. Statistical analysis

"SPSS 15.0 for Windows" program was used for statistical evaluation. Normal distribution of data was checked with the Kolmogorov-Smirnov test. Measurable (quantitative) data were defined as x ± SD. The difference between the two groups was examined using the Student *t*-test or Mann-Whitney *U* test Countable data (qualitative) were defined as percentages, and statistical analysis between groups was performed with the chi-square test. The sensitivity and specificity of the diagnostic criteria were calculated. The significance level in the evaluation was taken as $p < 0.05$. Receiver Operating Characteristic (ROC) analysis was performed to find the threshold ADC value for the characterization of the lesions.

Table 2
Demographic distribution of the groups.

	Hydatid Cyst	Simple Cyst	p
Age (years)	36.8 ± 20.2 (8–71)	58.5 ± 11.9 (32–79)	**<0.05**
Sex (F/M)	16/26	11/11	0.360
Size (mm)	70.6 ± 38.3 Type 1: 85.2 ± 45.4 Type 2: 47.7 ± 15.9 Type 3: 63.9 ± 23.8	33.8 ± 15.5	**<0.05**
Type (n)	**82** Type 1: 41 Type 2: 20 Type 3: 21	**40**	

Bold texts indicate hydatid and simple cyst numbers in the table.

3. Results

The mean age of 42 patients with hepatic hydatid cyst was 36.8 ± 20.2 years (between 8–71), and the mean age of 22 patients with liver simple cyst was 58.5 ± 11.9 years (between 32–79). While 16 (38.1 %) of the hydatid cyst cases were male and 26 (61.9 %) were female, 11 (50 %) of the simple cyst cases were male and 11 (50 %) were female. There was a statistically significant difference in age distribution between the two groups ($p < 0.05$), but no difference in terms of gender ($p > 0.05$). Of the 122 lesions, 40 were simple cysts and 82 were hydatid cysts (type 1: 41, type 2: 20, type 3: 21). The demographic characteristics of the groups are given in Table 2.

The average size of simple cysts was 33.8 ± 15.5 mm (20–94 mm). The mean size of all hydatid cysts was 70.6 ± 8.3 mm (20–230 mm). The average size was 85.2 ± 45.4 mm for type 1 hydatid cysts, 47.7 ± 15.9 mm for type 2 hydatid cysts, and 63.9 ± 23.8 mm for type 3 hydatid cysts. Paired comparisons were made between these groups in order to determine which groups caused the significant statistical difference in terms of mean dimension values. A statistically significant difference was found between the simple cyst and hydatid cyst groups ($p < 0.05$) (Table 2).

3.1. DWI and ADC findings

Signal intensity in b600 DWIs was compared with normal liver parenchyma and evaluated as isointense, moderately hyperintense, hyperintense in the periphery, and hyperintense. While 31 (77.5 %) lesions were moderately hyperintense in the simple cyst group, 19 (23.2 %) lesions were moderately hyperintense in the hydatid cyst group (Fig. 1). Peripheral hyperintensity was not observed in the simple cyst group, whereas peripheral hyperintensity was observed in 53 (64.6 %) lesions in the hydatid cyst group (Fig. 2). A statistically significant difference was found between the simple cyst and hydatid cyst groups according to the signal intensity ($p < 0.05$) (Table 3).

When the average ADC (b600) values are evaluated according to cyst types, the average value is $3.15 \pm 0.32 \times 10^{-3}$ s/mm^2 for type 1 hydatid

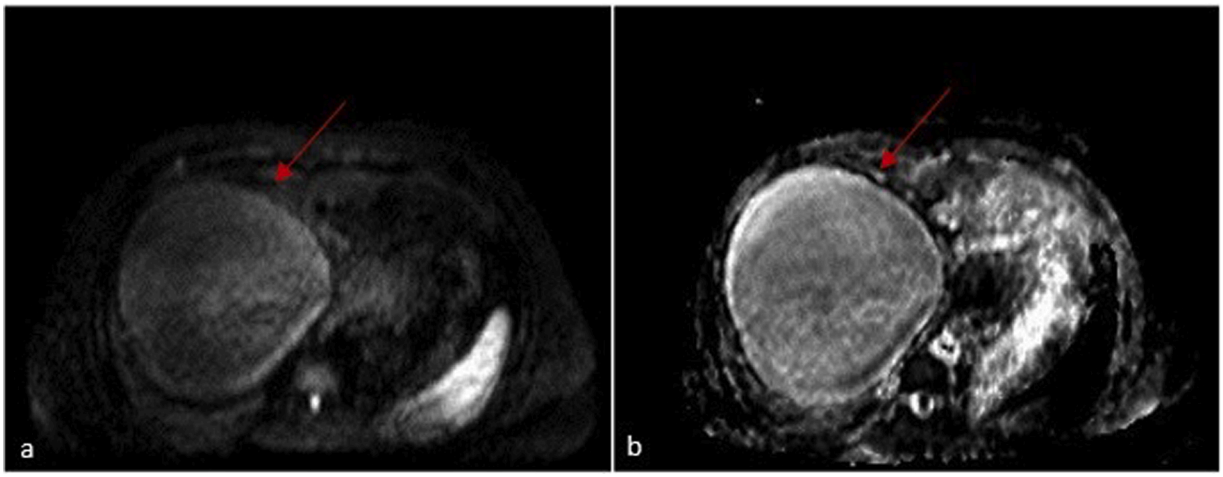

Fig. 1. Type 1 hydatid cyst with b600 value on DWI (a) and ADC map (b); moderate hyperintensity is more prominent in the periphery compared to the liver parenchyma. ADC value; 3.10 × 10-3 s / mm^2.

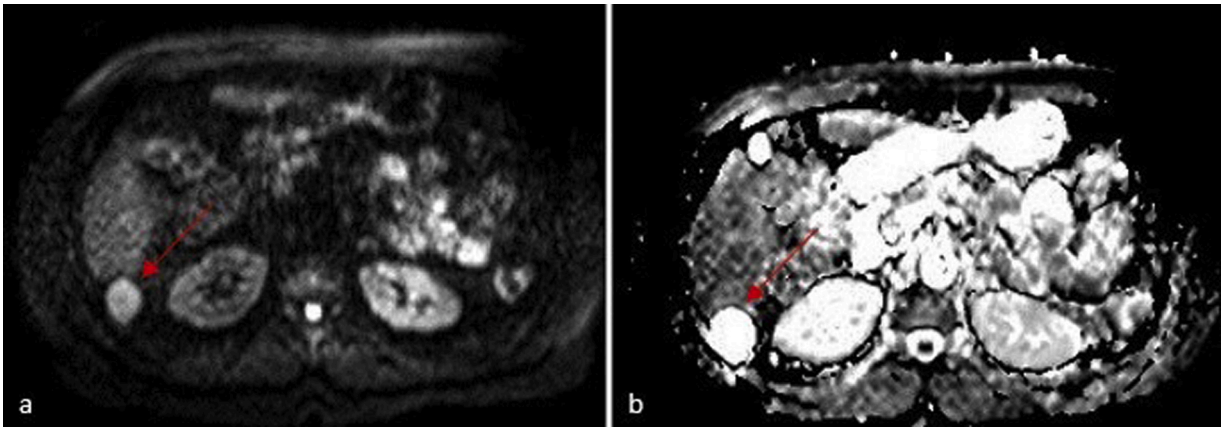

Fig. 2. A simple cyst with b600 value on DWI (a) and ADC map (b); moderate hyperintensity is observed compared to the liver parenchyma. ADC value; 3.95 × 10-3 s / mm^2.

Table 3
Signal characteristics of hydatid and simple cysts in b600 DWI and average ADC (b600) values.

	DWI				ADC
	Isointense	Moderately hyperintense	Moderately hyperintense in the periphery	Hyperintense	b600 (x10^{-3} s/mm^2)
Simple Cyst (n/%)	**2** (5)	**31** (77.5)	**0** (0)	**7** (17.5)	**3.91 ± 0.51**
Hydatid Cyst (n/%)	**6** (7.3)	**19** (23.2)	**53** (64.6)	**4** (4.9)	**3.07 ± 0.41**
Type 1	0	1	40	0	3.15 ± 0.32
Type 2	4	11	1	4	3.13 ± 0.57
Type 3	2	7	12	0	2.88 ± 0.33

Bold texts indicate hydatid and simple cyst numbers in the table.

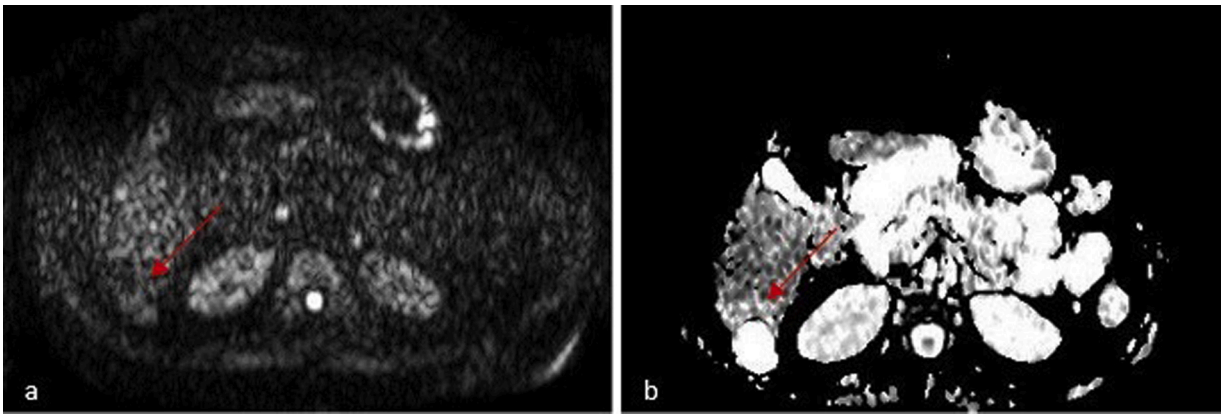

Fig. 3. Simple cyst with b1000 DWI (a) and ADC map (b). It is isointense on DWI compared to the liver parenchyma. ADC value; 3.60 × 10-3 s / mm^2.

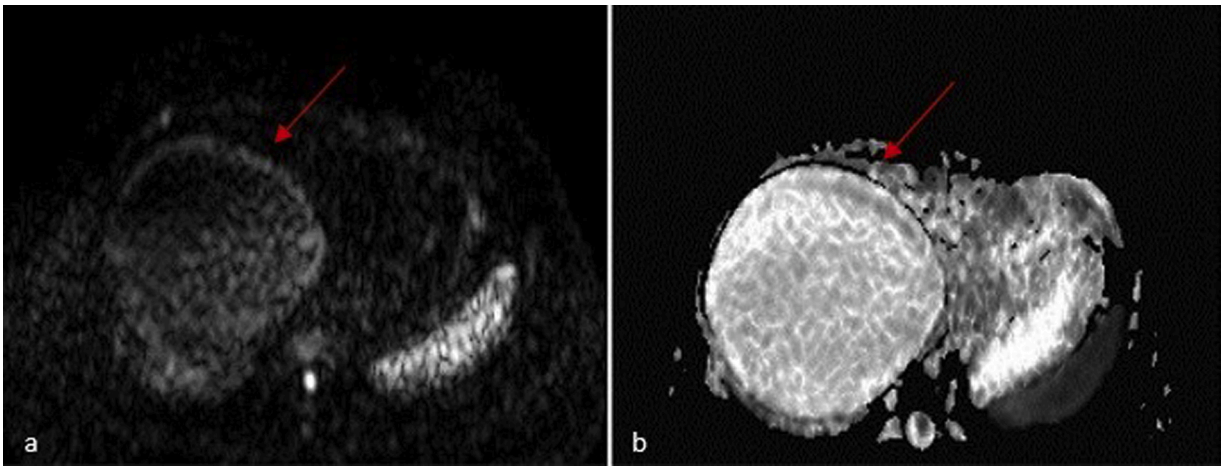

Fig. 4. Type 1 hydatid cyst with b1000 DWI (a) and ADC map (b). The cyst is moderately hyperintense in the periphery and isointense in the center. ADC value; 3.05 × 10-3 s / mm^2.

cysts, 3.13 ± 0.57 × 10^{-3} s/mm^2 for type 2 hydatid cysts, and 2.88 ± 0.33 × 10^{-3} s/mm^2 for type 3 hydatid cysts. The mean value for all hydatid cysts was 3.07 ± 0.41 × 10^{-3} s/mm^2. The ADC (b600) mean value of simple cysts was found to be 3.91 ± 0.51 × 10^{-3} s/mm^2 (Table 3). Paired comparisons were made between the groups in order to determine which groups caused the statistically significant difference in average ADC (b600) values. A statistically significant difference was found between all types of hydatid cysts and simple cysts and between

Table 4
Signal characteristics of hydatid and simple cysts in b1000 DWI and average ADC (b1000) values.

	DWI				ADC
	Isointense	Central isointense, moderately hyperintense in the periphery	Moderately hyperintense	Hyperintense	b1000 (x10^{-3} s/mm^2)
Simple Cyst (n/%)	34 (85)	1 (2.5)	4 (10)	1 (2.5)	3.43 ± 0.29
Hydatid Cyst (n/%)	24 (29.3)	44 (53.6)	10 (12.2)	4 (4.9)	2.99 ± 0.38
Type 1	8	33	0	0	3.01 ± 0.37
Type 2	10	1	5	4	3.02 ± 0.45
Type 3	6	10	5	0	2.90 ± 0.32

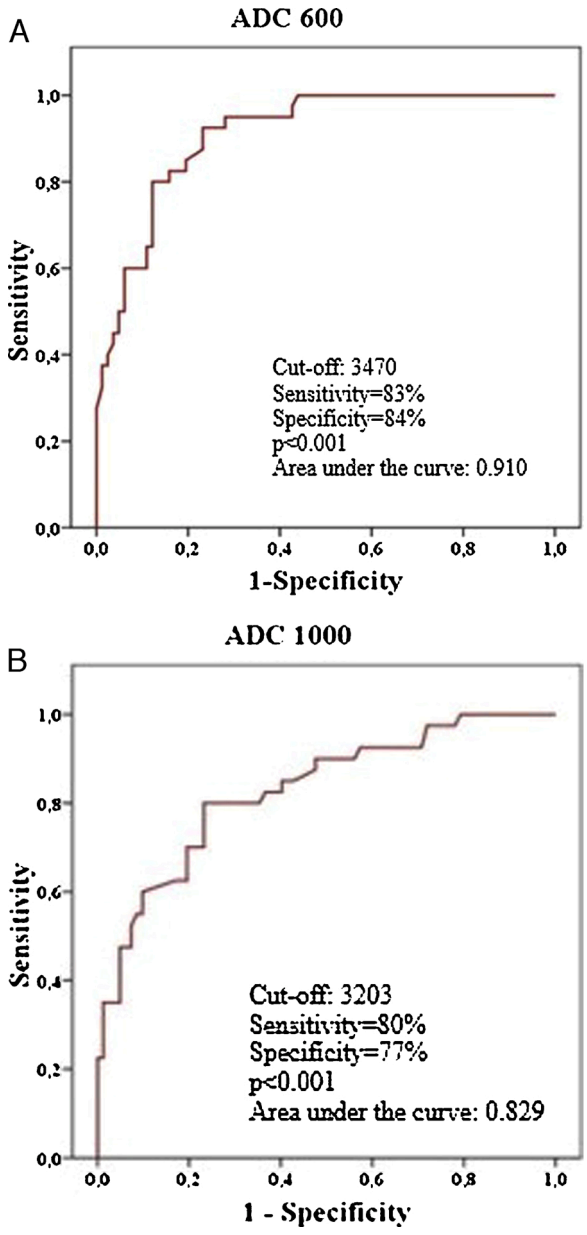

Fig. 5. ROC curves for differentiation between hydatid cysts and simple cysts in b600 (a) and b1000 (b).

type 1 and type 3 hydatid cysts ($p < 0.05$).

The signal intensity of liver hydatid cysts and simple cysts in b1000 DWIs was compared with the normal liver parenchyma and evaluated as isointense, central isointense plus moderately hyperintense in the periphery, moderately hyperintense and hyperintense. While 34 (85 %) lesions were isointense in the simple cyst group (Fig. 3), 24 (29.3 %) lesions were moderately isointense in the hydatid cyst group (Fig. 4). In the simple cyst group, peripheral hyperintensity was observed in 1 (2.5 %) lesion, while in the hydatid cyst group, peripheral hyperintensity was observed in 44 (53.6 %) lesions. A statistically significant difference was found between the simple cyst and hydatid cyst groups according to the signal intensity ($p < 0.05$) (Table 4).

When the average ADC (b1000) values according to the types are evaluated, the average value was $3.01 \pm 0.37 \times 10^{-3}$ mm^2/s for type 1 hydatid cysts, 3.01 ± 0.3 s/mm^2 for type 2 hydatid cysts, $2.90 \pm 0.32 \times 10^{-3}$ s/mm^2 for type 3 hydatid cysts, while the mean value for all hydatid cysts was $2.99 \pm 0.38 \times 10^{-3}$ s/mm^2. The ADC (b1000) mean value for simple cysts was $3.43 \pm 0.29 \times 10^{-3}$ s/mm^2.

Table 5
Signal characteristics of hydatid and simple cysts in the FLAIR sequence.

	FLAIR		
	Hypointense	Izointense	Hyperintense
Simple Cyst (n/%)	**33** (82.5)	**2** (5)	**5** (12.5)
HydatidCyst (n/%)	**56** (70)	**8** (10)	**18** (20)
Type 1	39	0	2
Type 2	1	6	13
Type 3	16	2	3

Bold texts indicate hydatid and simple cyst numbers in the table.

Paired comparisons were made between the groups in order to determine which groups caused the statistically significant difference in mean ADC (b1000) values. A statistically significant difference was found between all types of hydatid cysts and simple cysts ($p < 0.05$) (Table 4).

B600 and b1000 ROC analyses were performed to find the threshold value for differentiation between hydatid cyst and simple cyst (Fig. 5a, b).

3.2. FLAIR findings

The signal intensity was evaluated as hypointense, isointense, and hyperintense by comparing with normal liver parenchyma (Table 5). Paired comparisons were made between the groups in order to determine which groups caused the statistically significant difference in signal intensity. A statistically significant difference was found between type 2 hydatid cysts and type 1, type 3 hydatid cysts and simple cysts ($p < 0.05$) (Fig. 6).

4. Discussion

Hydatid cyst is most common in the 3rd and 4th decade and is localized at a rate of 50–70 % in the liver, 11–17 % in the lungs, 2.4–5.3 % in soft tissues, 0.5–3 % in the heart, 5 % in the pericardium, and 0.5–4.7 % in muscle and subcutaneous tissues [16,17]. Hydatid cysts in the liver can be millimetric or can reach 50 cm in size. Average size is 5−6 cm [18–20]. Simple liver cysts originate from intrahepatic bile ducts and are commonly seen in the 5th-7th decades. Size is approximately 3 cm [21]. In our study, the larger size of hydatid cysts compared to simple cysts was attributed to the viability of the hydatid cyst walls and continuous fluid production. The appearance of simple cysts at a later age was attributed to their smaller size and being asymptomatic.

DWI is an MRI technique that can measure the diffusion of water molecules in biological tissues quantitatively and noninvasively. High b values (greater than 400 s/mm^2) should be selected for accurate ADC measurements in abdominal evaluation [11,22,23]. The most suitable b values were reported as b500−600 sec/mm^2 [24]. Normal liver parenchyma has a short T2 relaxation time, so the b value should not be greater than 1000s/mm^2 [25]. Inan et al. [13] found a significant difference in b1000 values but not a significant difference in b500 values in their study of hydatid cysts and simple cysts. For these reasons, b600 and b1000 values were used in this study.

Studies show that the ADC values for benign liver lesions are significantly higher than for malignant lesions. This difference was attributed to benign lesions often having lower cellularity than malignant lesions [26–28]. There are limited studies in the literature regarding the use of DWI for the differential diagnosis and classification of hydatid cysts from other cystic lesions that are benign liver lesions [29,30]. Oruc et al. [14] used b1000 value in their study with hydatid cyst, abscess and simple cyst, and ADC values were 2.84 ± 0.38, 3.05 ± 0.17, 1.70 ± 0.44, 2.92 ± 0.63, 1.26 ± 0.42, and $3.08 \pm 0.76 \times 10^{-3}$ s/mm^2, respectively for type 1, 3, 4, 5 hydatid cyst, abscess, and simple cyst. While simple cysts and abscesses can be distinguished from type 1-2-3 hydatid cysts by ADC values, type 1 and type 3 hydatid cysts cannot be differentiated from simple cysts. The low

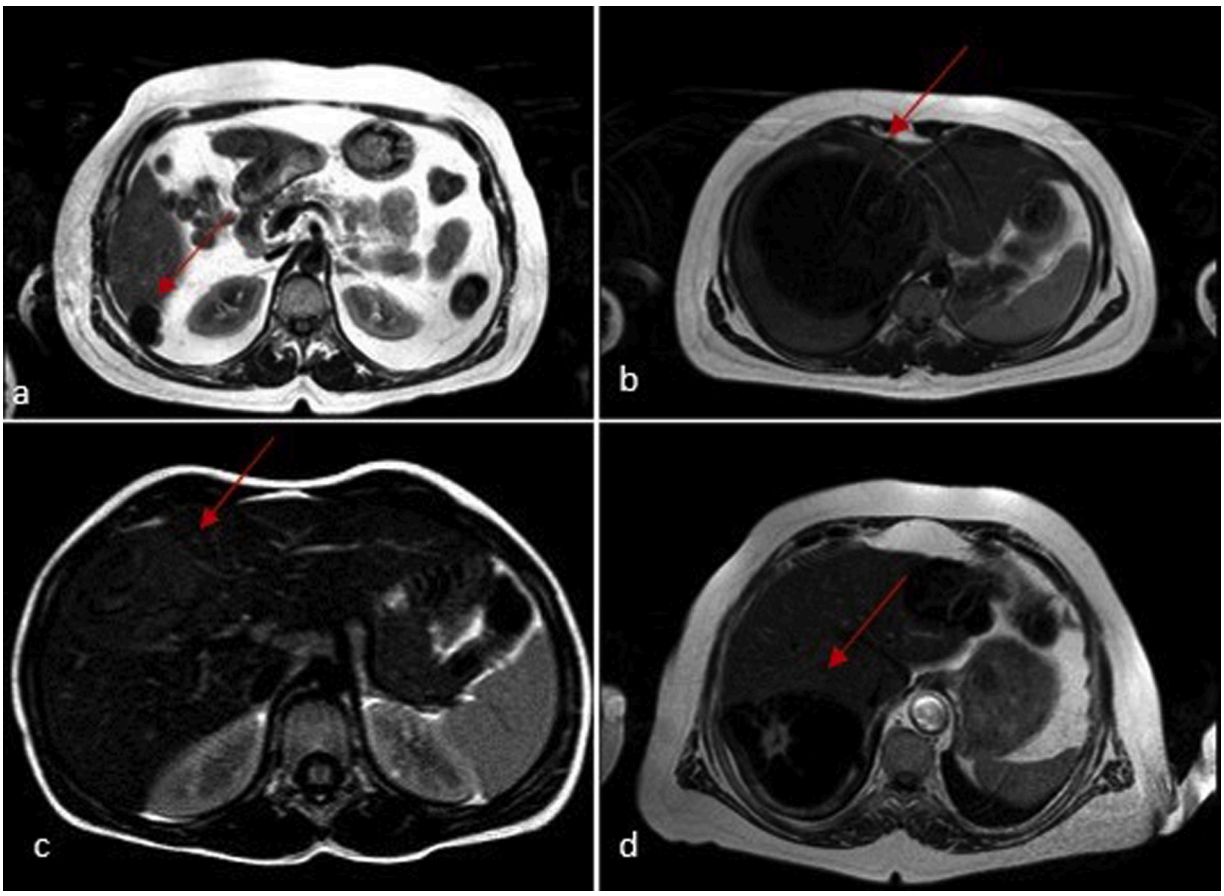

Fig. 6. FLAIR sequence (a) simple cyst, (b) type 1 hydatid cyst, (c) type 2 hydatid cyst, (d) type 3 hydatid cyst. While simple cysts, type 1 and type 3 hydatid cysts are hypointense with suppression, type 2 hydatid cyst is not suppressed and is observed as hyperintense.

number of cases and the absence of a type 2 hydatid cyst case were stated as serious limitations of the study.

Çeçe et al. [29] used the b1000 value in their study and ADC values were 2.48 ± 0.16, 2.80 ± 0.34, 2.70 ± 0.34, 2.02 ± 0.01 and 2.18 ± 0.1 × 10^{-3} mm^2/s for type 1, 2, 3, 4 and 5 hydatid cysts, respectively. In terms of mean ADC values, a statistically significant difference was found between types 1, 2, 3, and types 4, 5, and the sensitivity was 90.9 % and specificity was 90.9 %.

Sonmez et al. [30] found no statistically significant difference between b0 and b500 in their study with type 1 and 2 hydatid cysts and simple cysts. ADC values at b1000 were calculated as 2.22 ± 0.24 × 10^{-3} mm^2/s for all hydatid cysts and 2.67 ± 0.04 × 10^{-3} mm^2/s for simple cysts. According to the ADC values, a distinction was made between the whole hydatid cyst group and simple cysts, with sensitivity of 60 % and specificity of 95 %.

In our study, when the threshold value in ROC analysis for b600 was considered as 3.7 × 10^{-3} mm^2/sec, sensitivity was found as 83 % and specificity was 84 %. With b1000, when the threshold value was accepted as 3.2 × 10^{-3} mm^2/sec in ROC analysis, sensitivity was found to be 80 % and specificity was 77 %. It was shown that ADC values are lower in hydatid cysts compared to simple cysts. This difference is based on the serous fluid content of simple cysts; the value for hydatid cysts was attributed to their denser content consisting of scolex, sodium chloride, proteins, glucose, ions, lipids, and polysaccharides [31,32].

The numerical differences between the ADC values in different studies are due to variations in in the b values used, the device and parameters used, gradient changes, and shooting technique used [33]. However, as in both studies by Çeçe et al. and Sönmez et al., the common point was that ADC values decrease as the cyst content increases, as we found in our study.

As one of the routines in neuroradiological imaging, the long duration of the FLAIR sequence was a disadvantage in abdominal MRI applications, but it has become applicable with fast sequences developed recently [34,35]. In the literature, there are few studies about the FLAIR sequence in abdominal MR applications [36–38]. Without contrast studies, the distinction between hemangioma and simple cyst, which are benign liver lesions, cannot be always reliably made.

Sasaki et al. [37] investigated the contribution of the FLAIR sequence to differential diagnosis in a study conducted with patients with simple cysts and hemangiomas and reported that 96.3 % of simple cysts were hypointense compared to liver parenchyma, and 98.2 % of hemangiomas were hyperintense compared to liver parenchyma. The appearance of simple cysts that are not monitored as hypointense may be due to protein or hemorrhagic content. In another study, simple cyst and metastases were compared, and 97.3 % of simple cysts were hypointense, 94.9 % of metastases were hyperintense, and the FLAIR sequence was a safe modality for differential diagnosis [36]. In these two studies, the TI value was selected as 2265 ms, and the fact that simple cysts could be distinguished with the FLAIR sequence was attributed to the difference in the TI values of the lesions [39,40]. Naganawa et al. [38] chose the TI value as 920 ms for the FLAIR sequence and stated that simple cysts were suppressed, unlike hepatocellular carcinoma, hemangioma, and liver metastases, and were observed as hypointense compared to liver parenchyma.

In the literature, there is no study conducted with FLAIR sequence for hydatid cysts. Our work on this subject is a unique study. In our study, 33 (82.5 %) simple cysts became hypointense compared to liver parenchyma by being suppressed on FLAIR sequence, while 7 (17.5 %) simple cysts were observed as iso-hyperintense and not suppressed. Five (12.5 %) of the simple non-suppressed cysts were proven to be

hyperintense on T1W images and surgically hemorrhagic. Two simple cysts were observed to be isointense compared with the liver on FLAIR sequence. Of hydatid cysts, 56 (70 %) were suppressed on FLAIR sequence as with simple cysts, and hypointense compared to liver parenchyma. While 55 (68.8 %) of the suppressed hydatid cysts were type 1 and type 3 hydatid cysts, 19 (23.8 %) of the non-suppressed hydatid cysts were type 2 hydatid cysts. A statistical distinction could be made between type 2 hydatid cysts from type 1 and type3 hydatid cysts and simple cysts. In type 2 hydatid cysts, the pressure inside the cyst decreases, and the germinative membrane is separated, its internal structure changes and begins to degenerate, and bile leakage may occur into the cyst [41–43]. The WHO named this period the transitional phase between active (types 1 and 3) and inactive phases (types 4 and 5) [4]. The different characteristics of type 2 hydatid cysts compared to type 1 and 3 hydatid cysts and simple cysts on the FLAIR sequence are attributed to the transitional phase.

4.1. Limitations

The parallel imaging method or respiratory triggered imaging method, which are techniques to increase image quality, were not used. Therefore, signal-to-noise ratio was low. Anatomical details decreased especially on DWIs with b1000 value; therefore, lesions smaller than 2 cm were not included in the study. Type 4 and type 5 hydatid cysts were not included in the study. The distribution of the number of patients between the groups was not equal.

4.2. Conclusion

Simple cyst and hydatid cyst (type 1- 2-3) distinctions can be made with ADC measurements at b600 and b1000 values. Simple cysts and hydatid cysts (type 1- 2-3) are isointense on DWI with b1000, and peripheral moderate hyperintensity was observed in contrast to hydatid cysts. The simple cyst and hydatid cyst (type 1, 2 and 3) were hypointense and could not be differentiated but type 2 hydatid cyst was hyperintense on FLAIR.

Ethical approval

Institutional Review Board approval was obtained from Erciyes University, School of Medicine, Kayseri, Turkey (No: 2012/79).

Funding source

This research did not receive any specific grant from funding agencies in the public, commercial, or not-for-profit sectors.

CRediT authorship contribution statement

Kursad Yalcinoz: Resources, Conceptualization, Methodology, Formal analysis, Investigation, Writing - original draft. **Turkan Ikizceli:** Formal analysis, Data curation, Writing - review & editing. **Servet Kahveci:** Data curation, Investigation, Methodology. **Okkes Ibrahim Karahan:** Supervision, Project administration.

Declaration of Competing Interest

The authors report no declarations of interest.

Acknowledgments

Authors would like to thank the patients for their munificence in contributing to this study.

References

[1] A. Kabaalioğlu, K. Karaali, A. Apaydin, M. Melikoğlu, T. Sindel, E. Lüleci, Ultrasound-guided percutaneous sclerotherapy of hydatid liver cysts in children, Pediatr. Surg. Int. 16 (2000) 346–350, https://doi.org/10.1007/s003830000356.
[2] J. Dadoukis, O. Gamvros, H. Aletras, Intrabiliary rupture of the hydatid cyst of the liver, World J. Surg. 8 (1984) 786–790, https://doi.org/10.1007/BF01655782.
[3] H.A. Gharbi, W. Hassine, M.W. Brauner, K. Dupuch, Ultrasound examination of the hydatic liver, Radiology 139 (1981) 459–463, https://doi.org/10.1148/radiology.139.2.7220891.
[4] WHO Informal Working Group, International classification of ultrasound images in cystic echinococcosis for application in clinical and field epidemiological settings, Acta Trop. 85 (2003) 253–261, https://doi.org/10.1016/s0001-706x(02)00223-1.
[5] A.A. Abdel Razek, O. El-Shamam, N. Abdel Wahab, Magnetic resonance appearance of cerebral cystic echinococcosis: World Health Organization (WHO) classification, Acta radiol. 50 (2009) 549–554, https://doi.org/10.1080/02841850902878161.
[6] A.A. Abdel Razek, A. Watcharakorn, M. Castillo, Parasitic diseases of the central nervous system, Neuroimaging Clin. N. Am. 21 (2011) 815–841, https://doi.org/10.1016/j.nic.2011.07.005.
[7] K.A. Alghofaily, M.B. Saeedan, I.M. Aljohani, M. Alrasheed, S. McWilliams, A. Aldosary, M. Neimatallah, Hepatic hydatid disease complications: review of imaging findings and clinical implications, Abdom. Radiol. (NY) 42 (2017) 199–210, https://doi.org/10.1007/s00261-016-0860-2.
[8] M. El-Tahir, M.F. Omojola, T. Malatani, A.H. Al-Saigh, O.A. Ogunbiyi, Hydatid disease of the liver: evaluation of ultrasound and computed tomography, Br. J. Radiol. 65 (1992) 390–392, https://doi.org/10.1259/0007-1285-65-773-390.
[9] S. Singh, S.V. Gibikote, Magnetic resonance imaging signal characteristics in hydatid cysts, Australas. Radiol. 45 (2001) 128–133, https://doi.org/10.1046/j.1440-1673.2001.00892.x.
[10] M.F. Müller, P. Prasad, B. Siewert, M.A. Nissenbaum, V. Raptopoulos, R. R. Edelman, Abdominal diffusion mapping with use of a whole-body echo-planar system, Radiology 190 (1994) 475–478, https://doi.org/10.1148/radiology.190.2.8284402.
[11] K. Tokat, T. Ikizceli, The role of Diffusion-Weighted Imaging and Apparent Diffusion Coefficient maps in characterization of solid renal lesions, Phnx Med J. 2 (2020) 138–144, https://doi.org/10.38175/phnx.806582.
[12] M.K. Shin, S.J. Song, S.B. Hwang, H.P. Hwang, Y.J. Kim, W.S. Moon, Liver fibrosis assessment with Diffusion-Weighted Imaging: Value of liver Apparent Diffusion Coefficient normalization using the spleen as a reference organ, Diagnostics (Basel) 28 (2019) 107, https://doi.org/10.3390/diagnostics9030107.
[13] N. Inan, A. Arslan, G. Akansel, Y. Anik, H.T. Sarisoy, E. Ciftci, A. Demirci, Diffusion-weighted imaging in the differential diagnosis of simple and hydatid cysts of the liver, AJR Am. J. Roentgenol. 189 (2007) 1031–1036, https://doi.org/10.2214/AJR.07.2251.
[14] E. Oruç, N. Yıldırım, N.B. Topal, S. Kılıçturgay, S. Akgöz, G. Savcı, The role of diffusion-weighted MRI in the classification of liver hydatid cysts and differentiation of simple cysts and abscesses from hydatid cysts, Diagn. Interv. Radiol. 16 (2010) 279–287, https://doi.org/10.4261/1305-3825.DIR.2807-09.2.
[15] M. Essig, M.V. Knopp, J. Debus, S.O. Schönberg, F. Wenz, H. Hawighorst, G. van Kaick, Fluid-attenuated-inversion-recovery (FLAIR) imaging in the diagnosis of cerebral gliomas and metastases, Radiologe 39 (1999) 151–160, https://doi.org/10.1007/s001170050490. German.
[16] K.N. Jee, Hepatic hydatid cyst, Korean J. Intern. Med. 30 (2015) 554–555, https://doi.org/10.3904/kjim.2016.425.
[17] G. Salamone, L. Licari, B. Randisi, N. Falco, R. Tutino, A. Vaglica, R. Gullo, C. Porello, G. Cocorullo, G. Gulotta, Uncommon localizations of hydatid cyst. Review of the literatüre, G Chir 37 (2016) 180–185, https://doi.org/10.11138/gchir/2016.37.4.180.
[18] S. Aksoy, I. Erdil, E. Hocaoglu, E. Inci, G.T. Adas, O. Kemik, R. Turkay, The Role of Diffusion-Weighted Magnetic Resonance Imaging in the differential diagnosis of simple and hydatid cysts of the liver, Niger. J. Clin. Pract. 21 (2018) 212–216, https://doi.org/10.4103/njcp.njcp_296_16.
[19] B.V. Czermak, O. Akhan, R. Hiemetzberger, B. Zelger, W. Vogel, W. Jaschke, M. Rieger, S.Y. Kim, J.H. Lim, Echinococcosis of the liver, Abdom. Imaging 33 (2008) 133–143, https://doi.org/10.1007/s00261-007-9331-0.
[20] M. Federle, T. Desser, V.S. Anne, A. Eraso, Diagnostic imaging abdomen, in: M. Federle (Ed.), Hepatobiliary and Pancreas, 1st ed., Amirsys, Utah, 2004, pp. 98–101, part II-2.
[21] Y. Nakamura, T. Higaki, Y. Akiyama, W. Fukumoto, K. Kajiwara, Y. Kaichi, Y. Honda, D. Komoto, F. Tatsugami, M. Iida, T. Ohmoto, S. Date, K. Awai, Diffusion-weighted MR imaging of non-complicated hepatic cysts: value of 3T computed diffusion-weighted imaging, Eur. J. Radiol. Open 3 (2016) 138–144, https://doi.org/10.1016/j.ejro.2016.07.001.
[22] T. Ichikawa, H. Haradome, J. Hachiya, T. Nitatori, T. Araki, Diffusion-weighted MR imaging with a single-shot echoplanar sequence: detection and characterization of focal hepatic lesions, AJR Am. J. Roentgenol. 170 (1998) 397–402, https://doi.org/10.2214/ajr.170.2.9456953.
[23] T. Namimoto, Y. Yamashita, S. Sumi, Y. Tang, M. Takahashi, Focal liver masses: characterization with diffusion-weighted echo-planar MR imaging, Radiology 204 (1997) 739–744, https://doi.org/10.1148/radiology.204.3.9280252.
[24] B. Taouli, V. Vilgrain, E. Dumont, J.L. Daire, B. Fan, Y. Menu, Evaluation of liver diffusion isotropy and characterization of focal hepatic lesions with two single-shot echo-planar MR imaging sequences: prospective study in 66 patients, Radiology 226 (2003) 71–78, https://doi.org/10.1148/radiol.2261011904.

[25] R. Turner, D. Le Bihan, J. Maier, R. Vavrek, L.K. Hedges, J. Pekar, Echo-planar imaging of intravoxel incoherent motion, Radiology 177 (1990) 407–414, https://doi.org/10.1148/radiology.177.2.2217777.
[26] M. Kanematsu, S. Goshima, H. Watanabe, H. Kondo, H. Kawada, Y. Noda, A. Aomatsu, N. Moriyama, Detection and characterization of focal hepatic lesions with diffusion-weighted MR imaging: a pictorial review, Abdom. Imaging 38 (2013) 297–308, https://doi.org/10.1007/s00261-012-9940-0.
[27] Y. Boulanger, M. Amara, L. Lepanto, G. Beaudoin, B.N. Nguyen, G. Allaire, M. Poliquin, V. Nicolet, Diffusion-weighted MR imaging of the liver of hepatitis C patients, NMR Biomed. 16 (2003) 132–136, https://doi.org/10.1002/nbm.818.
[28] T. Yoshikawa, H. Kawamitsu, D.G. Mitchell, Y. Ohno, Y. Ku, Y. Seo, M. Fujii, K. Sugimura, ADC measurement of abdominal organs and lesions using parallel imaging technique, AJR Am. J. Roentgenol. 187 (2006) 1521–1530, https://doi.org/10.2214/AJR.05.0778.
[29] H. Ceçe, M. Gündoğan, O. Karakaş, E. Karakaş, F.N. Boyacı, S. Yıldız, A. Ozgönül, E.Y. Karakaş, N. Cullu, A. Seker, The role of diffusion-weighted magnetic resonance imaging in the classification of hepatic hydatid cysts, Eur. J. Radiol. 82 (2013) 90–94, https://doi.org/10.1016/j.ejrad.2012.08.015.
[30] G. Sonmez, A.K. Sivrioglu, H. Mutlu, E. Ozturk, M. Incedayi, B. Karaman, C. C. Basekim, Is it possible to differentiate between hydatid and simple cysts in the liver by means of diffusion-weighted magnetic resonance imaging? Clin. Imaging 36 (2012) 41–45, https://doi.org/10.1016/j.clinimag.2011.03.005.
[31] I. Pedrosa, A. Saíz, J. Arrazola, J. Ferreirós, C.S. Pedrosa, Hydatid disease: radiologic and pathologic features and complications, Radiographics 20 (2000) 795–817, https://doi.org/10.1148/radiographics.20.3.g00ma06795.
[32] W.K. Volders, G. Gelin, R.C. Stessens, Best cases from the AFIP. Hydatid cyst of the kidney: radiologic-pathologic correlation, Radiographics 21 (2001) 255–260, https://doi.org/10.1148/radiographics.21.suppl_1.g01oc16s255.
[33] S. Goshima, M. Kanematsu, H. Kondo, R. Yokoyama, K. Kajita, Y. Tsuge, Y. Shiratori, M. Onozuka, N. Moriyama, Hepatic hemangioma: correlation of enhancement types with diffusion-weighted MR findings and apparent diffusion coefficients, Eur. J. Radiol. 70 (2009) 325–330, https://doi.org/10.1016/j.ejrad.2008.01.035.
[34] P. Maillard, O. Carmichael, D. Harvey, E. Fletcher, B. Reed, D. Mungas, C. DeCarli, FLAIR and diffusion MRI signals are independent predictors of white matter hyperintensities, AJNR Am. J. Neuroradiol. 34 (2013) 54–61, https://doi.org/10.3174/ajnr.A3146.
[35] M.G. Lee, Y.K. Jeong, J.C. Kim, E.M. Kang, P.N. Kim, Y.H. Auh, D. Chien, G. Laub, Fast T2-weighted liver MR imaging: comparison among breath-hold turbo-spin-echo, HASTE, and inversion recovery (IR) HASTE sequences, Abdom. Imaging 25 (2000) 93–99, https://doi.org/10.1007/s002619910019.
[36] K. Sasaki, K. Ito, T. Fujita, A. Shimizu, M. Yasui, M. Hayashida, M. Tanabe, N. Matsunaga, Small hepatic lesions found on single-phase helical CT in patients with malignancy: diagnostic capability of breath-hold, multisection fluid-attenuated inversion-recovery (FLAIR) MR imaging using a half-fourier acquisition single-shot turbo spin-echo (HASTE) sequence, J. Magn. Reson. Imaging 25 (2007) 129–136, https://doi.org/10.1002/jmri.20797.
[37] K. Sasaki, K. Ito, S. Koike, T. Fujita, H. Okazaki, N. Matsunaga, Differentiation between hepatic cyst and hemangioma: additive value of breath-hold, multisection fluid-attenuated inversion-recovery magnetic resonance imaging using half-Fourier acquisition single-shot turbo-spin-echo sequence, J. Magn. Reson. Imaging 21 (2005) 29–36, https://doi.org/10.1002/jmri.20226.
[38] S. Naganawa, H. Kawai, H. Fukatsu, Y. Sakurai, I. Aoki, S. Miura, T. Mimura, H. Kanazawa, T. Ishigaki, Diffusion-weighted imaging of the liver: technical challenges and prospects for the future, Magn. Reson. Med. Sci. 4 (2005) 175–186, https://doi.org/10.2463/mrms.4.175.
[39] M. Ohkawa, T. Katoh, S. Nakano, N. Fujiwara, Y. Mori, I. Hino, M. Tanabe, Use of fluid-attenuated inversion recovery (FLAIR) pulse sequences for differential diagnosis of hepatic hemangiomas and hepatic cysts, Acta Med. Okayama 51 (1997) 275–278, https://doi.org/10.18926/AMO/30785.
[40] Y. Tang, Y. Yamashita, T. Namimoto, M. Takahashi, Characterization of focal liver lesions with half-fourier acquisition single-shot turbo-spin-echo (HASTE) and inversion recovery (IR)-HASTE sequences, J. Magn. Reson. Imaging 8 (1998) 438–445, https://doi.org/10.1002/jmri.1880080226.
[41] L. Marti-Bonmati, F. Menor Serrano, Complications of hepatic hydatid cysts: ultrasound, computed tomography, and magnetic resonance diagnosis, Gastrointest. Radiol. 15 (1990) 119–125, https://doi.org/10.1007/BF01888753.
[42] J. Prousalidis, C. Kosmidis, K. Kapoutzis, E. Fachantidis, N. Harlaftis, H. Aletras, Intrabiliary rupture of hydatid cysts of the liver, Am. J. Surg. 197 (2009) 193–198, https://doi.org/10.1016/j.amjsurg.2007.10.020.
[43] M. Mio, Y. Fujiwara, K. Tani, T. Toyofuku, T. Maeda, T. Inoue, Quantitative evaluation of focal liver lesions with T1 mapping using a phase-sensitive inversion recovery sequence on gadoxetic acid-enhanced MRI, Eur. J. Radiol. Open 8 (2020), 100312, https://doi.org/10.1016/j.ejro.2020.100312.